International Conference on Automotive Composites
ICAutoC 2016
A. Elmarakbi and A.L. Araújo (Editors)

HIERARCHICAL MODELLING OF CARBON FIBRES GRAPHENE REINFORCED POLYMER COMPOSITE MATERIALS

Wiyao Leleng Azoti[a], Ahmed Elmarakbi[a], Hicham El-Hage[b] and Mustafa Elkady[b]

[a]Faculty of Applied Sciences, University of Sunderland, Sunderland, SR6 0DD, UK
[b]Lebanese International University Beirut, Lebanon
wiyao.azoti@sunderland.ac.uk
ahmed.elmarakbi@sunderland.ac.uk
hisham.elhage@liu.edu.lb
mostafa.kady@liu.edu.lb

Key words: Micromechanics, Tangent operators, 3-phases composite, Effective properties.

Summary: *This work aims to investigate the mechanical response of a hierarchical carbon fibres graphene reinforced polymer composite materials using analytical multiscale approaches. Therefore, a 2-phases graphene/polymer composite is computed under a boundary value problem. Mean-field homogenisation schemes for instance the Mori-Tanaka are applied to obtain the overall response. The modelling of 3-phases carbon fibres/graphene/polymer composite consists on a double-scale approach combining the 2-phases composite as matrix phase in which are embedded the carbon fibres. The derivation of the effective properties remains analytical-based micromechanics formalism. Numerical results obtained for thermoset as well as thermoplastic matrix derive the overall nonlinear stress-strain response and show the contribution of the graphene in the enhancement of mechanical properties.*

1 INTRODUCTION

Graphene based nanocomposites are widely used for enhancing the multifunctional response of composite materials [1-4]. Indeed, graphene-based polymers show substantial property enhancements at much lower loadings than polymer composites with conventional micron-scale fillers (such as glass or carbon fibres).
Nowadays, hierarchical advanced graphene based polymer composites constitute efficient materials to replace conventional composites in structural applications. In fact, hierarchical glass fibres GF reinforced graphene nanoplatelets GNP polypropylene PP composites [5] have shown that the combined effect of the two fillers of rather different size scales i.e., micro- and nanoscale can lead to significant improvement of the tensile modulus and impact strength while the dispersion of the nanofiller in the PP matrix promoted the formation of a stronger interface between the matrix and GF. Moreover, carbon fibres CF and GNPs reinforced poly-arylene ether nitrile (PEN) PEN/CF/GNP composites [6] have demonstrated the synergic effect of combining reinforcements to deliver excellent mechanical properties higher 1.7, 4.5 and 6.4 times larger than those of PEN/CF composites, PEN/GNP composites and PEN host, respectively.

In this work, a multiscale modelling is proposed for deriving the mechanical properties of hierarchical fibres reinforced graphene polymer matrix composites FRGPMCs. Graphene is considered as continuum platelets embedded within a rate-independent elasto plastic polymer matrix leading to a 2-phases composite. For the nonlinear phase, a Hill-type incremental linearization is used for rate equation leading to the derivation of the consistent tangent operator. Analytical based micromechanics formalism derives the effective non-linear response of the 2-phases composite. Next, carbon fibres are embedded in a matrix consisting on the 2-phases composite leading to the 3-phases composite.

2 THEORITICAL BACKGROUND

2.1 Mean field homogenisation

Let us consider a macroscopic homogeneous and microscopic heterogeneous material under the assumption of a representative volume element RVE. The associated boundary-value problems are formulated, in the terms of uniform macro field traction vector or linear displacement fields with body forces and inertia term neglected. The effective properties are given by:

$$C_{ijkl}^{eff} = \frac{1}{V}\int_{V} c_{ijmn}(r)\, A_{mnkl}(r) dV \tag{1}$$

Or in others terms

$$\boldsymbol{C}^{eff} = \sum_{I=0}^{N} f_I \boldsymbol{c}^I : \boldsymbol{A}^I \tag{2}$$

with $\boldsymbol{c}^I$, $\boldsymbol{A}^I$, f_I the uniform stiffness tensor, the strain concentration tensor and the volume fraction of phase I respectively. Using, the Eshelby's inclusion concept [7], the final expression of the global strain concentration tensor is given by an iterative procedure [8] such as:

$$\begin{cases} \boldsymbol{A}^I = \boldsymbol{a}^I : \left\langle \boldsymbol{a}^I \right\rangle^{-1} \\ \left(\boldsymbol{a}^I\right)_0 = \mathbf{I} \\ \left(\boldsymbol{a}^I\right)_{i+1} = \left(\mathbf{I} + \boldsymbol{T}^{II} : \Delta\boldsymbol{c}^I\right)^{-1} : \left(\mathbf{I} - \sum_{\substack{J=0 \\ J\neq I}}^{N} \boldsymbol{T}^{IJ} : \Delta\boldsymbol{c}^J : \left(\boldsymbol{a}^J\right)_i \right) \\ I = 0,1,2,3,.....,N \end{cases} \tag{3}$$

where $\boldsymbol{a}^I$ states for the local strain concentration tensor and $\Delta\boldsymbol{c}^J = \boldsymbol{c}^J - \boldsymbol{c}^0$. $\boldsymbol{T}^{IJ}$ represents the interaction tensor between inclusions. In the case where the interactions between inclusions are neglected i.e $\boldsymbol{T}^{IJ} = 0$ (most of cases in the open literature), the local concentration tensor $\boldsymbol{a}^I$ reads more simple expression:

$$\boldsymbol{a}^I = \left[\mathbf{I} + \boldsymbol{T}^{II} : \Delta\boldsymbol{c}^I\right]^{-1} = \left[\mathbf{I} + \mathbf{S} : \left(\boldsymbol{c}^0\right)^{-1} : \Delta\boldsymbol{c}^I\right]^{-1} \tag{4}$$

where $\mathbf{S}$ represents the Eshelby's tensor [7]. Its expression depends on the aspect ratio $\alpha = c/a$ of the ellipsoidal inclusion of semi-axis (a,b,c) and the material properties of the

surrounding matrix $\boldsymbol{c}^0$. Under the Mori-Tanaka MT [9] assumptions, the global strain concentration tensor of the matrix is expressed as [8, 10]:

$$\boldsymbol{A}^0 = \boldsymbol{a}^0 : \left\langle \boldsymbol{a}^I \right\rangle^{-1} = \left(f_0 \mathbf{I} + \sum_{I=1}^{N} f_I \boldsymbol{a}^I \right)^{-1} \tag{5}$$

leading to the effective MT properties through Eq. (2) such as:

$$\boldsymbol{C}^{MT} = \sum_{I=0}^{N} f_I \boldsymbol{c}^I \boldsymbol{A}^I = \left(f_0 \boldsymbol{c}^0 + \sum_{I=1}^{N} f_I \boldsymbol{c}^I \boldsymbol{a}^I \right) : \boldsymbol{A}^0 \tag{6}$$

2.2 Non-linear tangent operators

Within the RVE, let us assume that one or more phases behave elasto-plastically. Referring to the work by Doghri and Ouaar [11] at least two tangent operators can be defined: the "continuum" (or elasto-plastic) $\boldsymbol{C}^{ep}$ tangent operator, which is derived from the rate constitutive equation, and the "consistent" (or algorithmic) $\boldsymbol{C}^{alg}$ tangent operator, which is solved by a discretisation in the time interval $\left[t_n,\ t_{n+1}\right]$. These tangent operators are related to the rate of the constitutive equation as follows:

$$\begin{cases} \dot{\boldsymbol{\sigma}} = \boldsymbol{C}^{ep} : \dot{\boldsymbol{\varepsilon}} \\ \delta\boldsymbol{\sigma}_{n+1} = \boldsymbol{C}^{alg} : \delta\boldsymbol{\varepsilon}_{n+1} \end{cases} \tag{7}$$

They are derived from the classical J_2 flow rule:

$$\begin{cases} \boldsymbol{\sigma} = \boldsymbol{C}^{el} : \left(\boldsymbol{\varepsilon} - \boldsymbol{\varepsilon}^p \right) \\ f = \sigma_{eq} - R(p) - \sigma_Y \\ \dot{\boldsymbol{\varepsilon}}^p = \dot{p}\boldsymbol{N}, \quad \boldsymbol{N} = \dfrac{\partial f}{\partial \boldsymbol{\sigma}} = \dfrac{3}{2}\dfrac{dev(\boldsymbol{\sigma})}{\sigma_{eq}} \\ \sigma_{eq} = \left(\dfrac{3}{2} \boldsymbol{s} : \boldsymbol{s} \right)^{1/2} \end{cases} \tag{8}$$

The "continuum" (or elasto-plastic) $\boldsymbol{C}^{ep}$ tangent operator yields:

$$\begin{cases} \boldsymbol{C}^{ep} = \boldsymbol{C}^{el} - \dfrac{(2\mu)^2}{h} \boldsymbol{N} \otimes \boldsymbol{N} \\ h = 3\mu + \dfrac{dR}{dp} > 0 \end{cases} \tag{9}$$

while the "consistent" (or algorithmic) $\boldsymbol{C}^{alg}$ tangent operator is given by:

$$\begin{cases} \boldsymbol{C}^{alg} = \boldsymbol{C}^{ep} - \left(2\mu\right)^2 \Delta p \dfrac{\sigma_{eq}}{\sigma_{eq}^{tr}} \dfrac{\partial \boldsymbol{N}}{\partial \boldsymbol{\sigma}} \\ \dfrac{\partial \boldsymbol{N}}{\partial \boldsymbol{\sigma}} = \dfrac{1}{\sigma_{eq}} \dfrac{3}{2} \mathbf{I}^{dev} - \boldsymbol{N} \otimes \boldsymbol{N} \end{cases} \tag{10}$$

In equations (9) and (10), μ denotes the material shear modulus while $\boldsymbol{C}^{el}$ represents the elastic stiffness tensor and $R\left(p\right)$ is the hardening stress function with p the accumulated plastic strain. $\boldsymbol{N}$ represents the normal to the yield surface in the stress space. σ_{eq}^{tr} denotes a trial elastic predictor of σ_{eq}. $\mathbf{I}^{dev}$ stands for the deviatoric part of the fourth order symmetric identity tensor. The knowledge of internal variables such as Δp and σ_{eq}^{tr} is important for computing the algorithmic tangent operator in Eq. (10). A detailed procedure about the update of internal variables can be found in Azoti et al. [12]. $\boldsymbol{C}^{alg}$ will be later used to determine the overall composite behaviour using the MT scheme by Eq. (6).

3 HIERARCHICAL MODELLING

This modelling is concerned with the derivation of the effective properties for the hierarchical composite materials as shown by Figure 1. The multiscale strategy is set up around the following points:

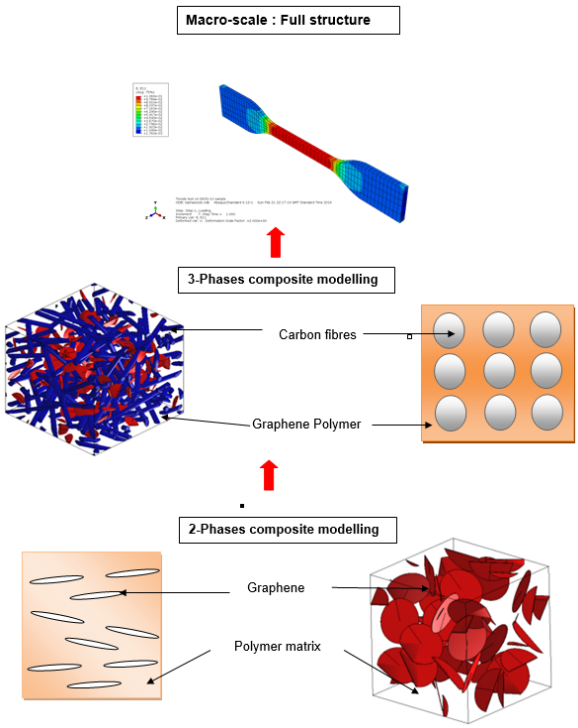

Figure1: Multiscale modelling of the hierarchical Short Glass fibres/Graphene platelets/polymer composite materials

- The modelling of *2-phases graphene/polymer* composite. The mechanical properties of the graphene which are widely derived at the atomistic scale [13, 14] are considered through graphene platelets GPL as continuum phases interacting with a rate-independent elasto plastic polymer matrix. The composite response is therefore computed under a boundary value problem by applying static or kinematic admissible loading. Mean-field homogenisation schemes for instance the Mori-Tanaka are applied to obtain the overall response.
- The modelling of *3-phases carbon fibres/graphene polymer* composite. It consists on a double-scale approach combining the *2-phases graphene/polymer* composite developed above as matrix phase in which are embedded the carbon fibres. The derivation of the effective properties remains analytical-based micromechanics formalism.
- the *full structure* simulation. At each Gauss integration point within a macro model, is implemented the above constitutive laws for *3-phases glass fibres/graphene polymer* composite using a User-defined Materials UMAT subroutine.

4 NUMERICAL RESULTS

Numerical results are conducted on the 3-phases composite. As matrix phase, thermosets (EM120, EM180) and thermoplastic (PA6) polymers are used while graphene platelets GPL (G2NAN) and short E-Glass fibres as well as carbon fibres are considered as reinforcements. Material properties used for analysis are gathered in Table1 and Table 2.
The following analysis cases are studied:

- Thermoset EM120 + G2NAN (0.78%)+carbon fibres (64%)
- Thermoset EM180 + G2NAN (0.61%)+carbon fibres (64%)
- Thermoplastic PA6 + G2NAN (1%) + short E-glass fibres (35%)

Carbon fibres		**Short E-Glass fibres**		**Graphene G2NAN**	
E_{CF}	ν_{CF}	E_{EGF}	ν_{EGF}	E_I	ν_I
230 GPa	0.2	85 GPa	0.23	700 GPa	0.22

Table 1: Reinforcement material properties

	Thermoplastic	**Thermoset-Epoxy**	
	PA6	***EM120***	***EM180***
Density	1.13 gm/cm3	1.14	1.17
Poisson's ratio	0.39	0.36	0.33
Young's Modulus	2000 MPa	3000 MPa	3200 MPa
Tensile Strength		85	90
Yield Stress	60.5 MPa	20 MPa	20 MPa
Hardening Modulus	63 MPa	90 MPa	90 MPa
Hardening Model	Power law	Power law	Power law
Hardening exponent	0.4	0.1	0.1

Table 2: Polymer matrix properties

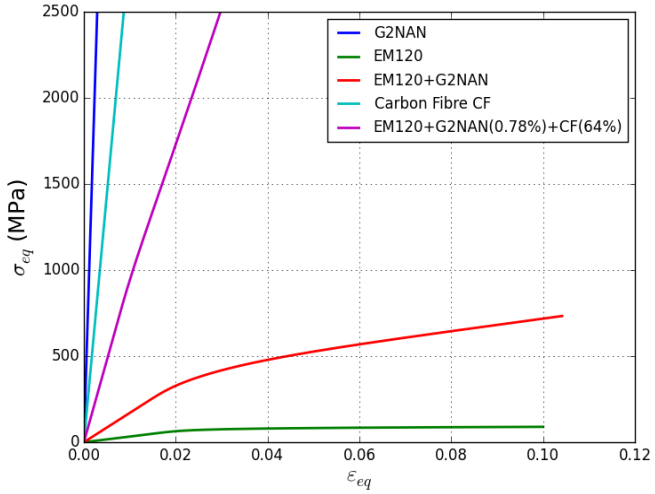

(a) EM120 + G2NAN (0.78%)+CF (64%)

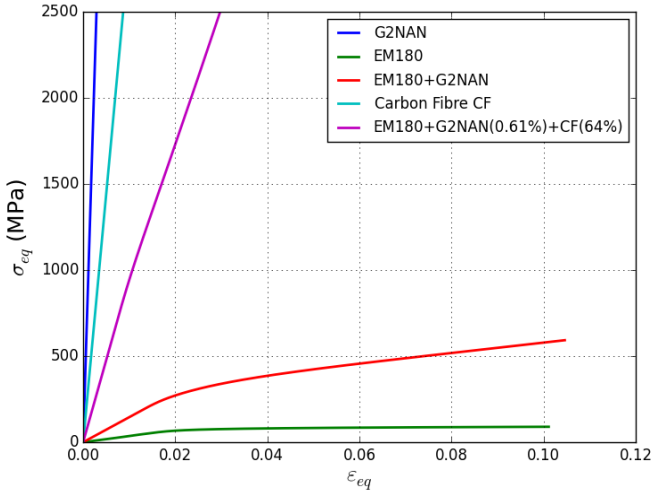

(b) EM180 + G2NAN (0.61%)+CF (64%)

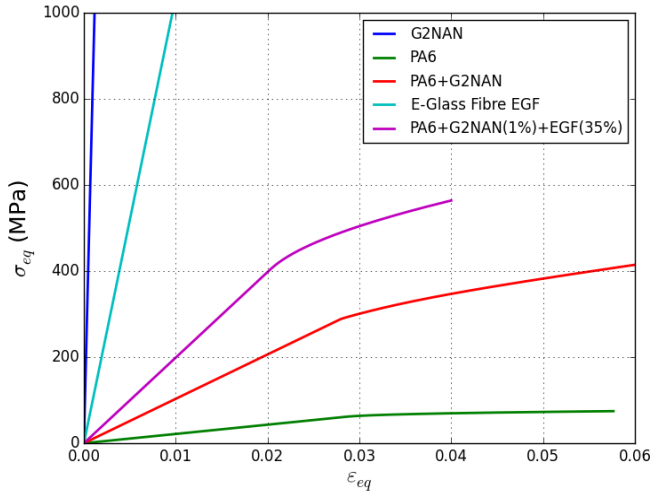

(c) PA6+ G2NAN (1%) + short E-glass fibres (35%)

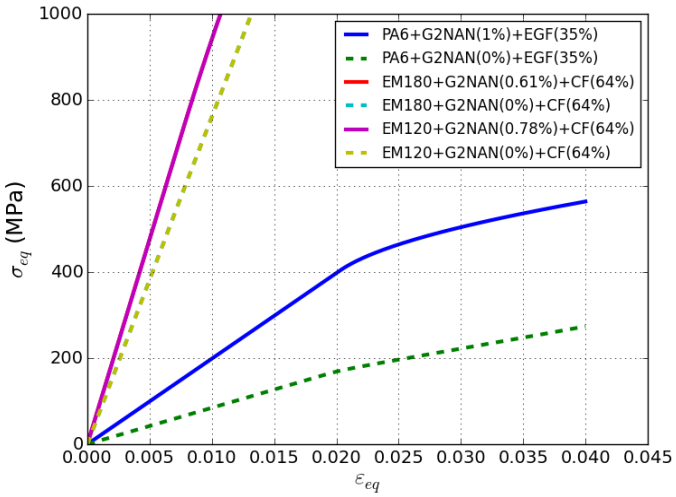

(d) Response comparison with and without graphene G2NAN

Figure 3: Effective stress-strain response of 3-phases composite under uniaxial loading

Results on Figure 3 shows the overall equivalent stress-strain response of the composite. The contribution of high volume fraction (64%) of carbons fibres in the composite response is depicted by. Figures 3(a) and (b) where the effective response shows a trend similar to that of the fibres. The 3-phases composite response is bonded between that of the fibres and the 2-phases composite which in turn is also bonded between the response of the GNP and that of the polymer matrix. In Figure 3(c), a trend similar to that of the matrix is obtained since a mean volume fraction of short E-Glass fibres is used (35%).

Also, the composite response, for all studied cases, is analysed with respect to the volume fraction of G2NAN in Figure 3(d). For composite without G2NAN ie 0% vol, it is observed a decrease in the overall behaviour. In addition, the stress strain response for that case quickly shifts to a linear response with the fibres volume fraction. For all studied cases, the presence of G2NAN has a significant impact in the enhancement of the overall response.

5 CONCLUSIONS

A nonlinear effective response has been proposed for modelling the hierarchical fibres reinforced graphene polymer matrix composites. For dealing with the material scale transition, the modelling strategy is based on mean-field homogenisation techniques. Therefore, micromechanics scheme for instance the Mori-Tanaka derives the effective response after the nonlinear consistent tangent operators are resolved from the classical J_2 flow rule. The developed methodology is versatile and can be used analytically as well as numerically through a user defined material UMAT. Numerical results that analyse different materials case, show the contribution of the graphene in the enhancement of the 3-phases composite materials.

Acknowledgments
The research leading to these results has received funding from the European Union Seventh

Framework Program under grant agreement no. **604391 Graphene Flagship**.

REFERENCES

[1] Mohammed A. Rafiee, Javad Rafiee, Iti Srivastava, Zhou Wang, Huaihe Song, Zhong-Zhen Yu, and Nikhil Koratkar. Fracture and fatigue in graphene nanocomposites. *Small*, 6 (2): 179–183, 2010.

[2] L. Monica Veca, Mohammed J. Meziani, Wei Wang, Xin Wang, Fushen Lu, Puyu Zhang, Yi Lin, Robert Fee, John W. Connell, and Ya-Ping Sun. Carbon nanosheets for polymeric nanocomposites with high thermal conductivity. *Advanced Materials*, 21 (20): 2088–2092, 2009.

[3] Zhen Xu and Chao Gao. In situ polymerization approach to graphene-reinforced nylon-6 composites. *Macromolecules*, 43 (16): 6716–6723, 2010.

[4] Wen Ling Zhang, Bong Jun Park, and Hyoung Jin Choi. Colloidal graphene oxide/polyaniline nanocomposite and its electrorheology. *Chem. Commun.*, 46: 5596–5598, 2010.

[5] Diego Pedrazzoli, Alessandro Pegoretti, and Kyriaki Kalaitzidou. Synergistic effect of graphite nanoplatelets and glass fibers in polypropylene composites. *Journal of Applied Polymer Science*, 132 (12), 2015.

[6] Xulin Yang, Zicheng Wang, Mingzhen Xu, Rui Zhao, and Xiaobo Liu. Dramatic mechanical and thermal increments of thermoplastic composites by multi-scale synergetic reinforcement: Carbon fiber and graphene nanoplatelet. *Materials & Design*, 44: 74 – 80, 2013.

[7] J. D. Eshelby. The determination of the elastic field of an ellipsoidal inclusion, and related problems. *Proceedings of the Royal Society of London. Series A, Mathematical and Physical Sciences*, 241 (1226): 376–396, 1957.

[8] P. Vieville, A. S. Bonnet, and P. Lipinski. Modelling effective properties of composite materials using the inclusion concept. general considerations. *Arch. Mech.*, 58 (3): 207–239, 2006.

[9] T Mori and K Tanaka. Average stress in matrix and average elastic energy of materials with misfitting inclusions. *Acta Metallurgica*, 21 (5): 571 – 574, 1973.

[10] W.L. Azoti, Y. Koutsawa, A. Tchalla, A. Makradi, and S. Belouettar. Micromechanics-based multi-site modeling of elastoplastic behavior of composite materials. *International Journal of Solids and Structures*, 59: 198 – 207, 2015.

[11] I. Doghri and A. Ouaar. Homogenization of two-phase elasto-plastic composite materials and structures: Study of tangent operators, cyclic plasticity and numerical algorithms. *International Journal of Solids and Structures*, 40 (7): 1681 – 1712, 2003.

[12] W.L. Azoti, A. Tchalla, Y. Koutsawa, A. Makradi, G. Rauchs, S. Belouettar, and H. Zahrouni. Mean-field constitutive modeling of elasto-plastic composites using two (2) incremental formulations. *Composite Structures*, 105: 256–262, 2013.

[13] J. Cho, J.J. Luo, and I.M. Daniel. Mechanical characterization of graphite/epoxy nanocomposites by multi-scale analysis. *Composites Science and Technology*, 67 (1112): 2399 – 2407, 2007.

[14] J.R. Xiao, B.A. Gama, and J.W. Gillespie Jr. An analytical molecular structural mechanics model for the mechanical properties of carbon nanotubes. *International Journal of Solids and Structures*, 42: 3075 – 3092, 2005.